PNAS RESEARCH ARTICLE | APPLIED BIOLOGICAL SCIENCES OPEN ACCESS

Dual ON/OFF-switch chimeric antigen receptor controlled by two clinically approved drugs

Greta Maria Paola Giordano Attianese[a], Sailan Shui[b,c], Elisabetta Cribioli[a], Melanie Triboulet[a], Leo Scheller[b,c], Morteza Hafezi[a], Patrick Reichenbach[a], Pablo Gainza[a,c], Sandrine Georgeon[b,c], Bruno E. Correia[b,c,1], and Melita Irving[a,1]

Affiliations are included on p. 10.

Edited by Carl June, University of Pennsylvania, Philadelphia, PA; received March 12, 2024; accepted September 7, 2024

The ability to remotely control the activity of chimeric antigen receptors (CARs) with small molecules can improve the safety and efficacy of gene-modified T cells. Split ON- or OFF-switch CARs involve the dissociation of tumor–antigen binding from T cell activation (i.e., CD3ζ) on the receptor (R-) and signaling (S-) chains, respectively, that either associate or are disrupted in the presence of a small molecule. Here, we have developed an inducible (i)ON-CAR comprising the anti-apoptotic B cell lymphoma protein 2 protein in the ectodomain of both chains which associate in the presence of venetoclax. We showed that inducible ON (iON)-CAR T cells respond to target tumors cells in the presence of venetoclax or the BH3 mimetic navitoclax in a dose-dependent manner, while there is no impact of the drugs on equivalent second generation-CAR T cells. Within 48 h of venetoclax withdrawal, iON-CAR T cells lose the ability to respond to target tumor cells in vitro as evaluated by Interferon-gamma (IFNγ) production, and they are reliant upon the presence of venetoclax for in vivo activity. Finally, by fusing a degron sequence to the endodomain of the iON-CAR S-chain we generated an all-in-one ON/OFF-switch CAR, the iONØ-CAR, down-regulated by lenalidomide within 4 to 6 for functionally inactive T cells (no IFNγ production) within 24 h. We propose that our remote-control CAR designs can reduce toxicity in the clinic. Moreover, the periodic rest of iON and iONØ-CAR T cells may alleviate exhaustion and hence augment persistence and long-term tumor control in patients.

chimeric antigen receptor | cancer | synthetic biology | T cell

Significance

T cells can be gene-modified with chimeric antigen receptors (CARs) to recognize and directly kill tumor cells. While CAR T cell therapy has been approved to treat some B cell malignancies, for nonhematological solid tumors toxicity and limited efficacy remain important obstacles. One approach to improve safety and T cell persistence is to incorporate an ON- or OFF-switch directly into the CAR that can be remotely regulated by administration of a small molecule. Here, we have developed an ON-CAR that can be induced by venetoclax as well as an all-in-one ON/OFF-CAR down-regulated by lenalidomide. Both of these small molecules are clinically approved and the switch components are of human origin thus reducing the risk of immunogenicity.

CAR T-cells have emerged as a game-changer in the treatment of some advanced liquid cancers, with curative responses now documented (1). While promising clinical outcomes have been reported for their use against nonhematological solid tumors (2) it is widely held that combinatorial or/and coengineering strategies [i.e., armored chimeric antigen receptor (CAR) T cells] will be needed to extend meaningful responses to more patients and cancer-types, and to prevent relapse (3). Examples include coadministration of low-dose irradiation (4–6) and further gene modifications of T cells to enforce the secretion of immunomodulatory molecules (7–9) or to abrogate the expression of exhaustion-associated genes (10). Undoubtedly, such next-generation CAR therapies will increase the risk of adverse events in patients which, including cytokine release syndrome (CRS) and neurotoxicity (11), are common and consequential for second generation (2G)-CAR T cells as a monotherapy (12). Indeed, predicting the appropriate dose of CAR T cells for patients is challenging due to variability in tumor burden, differences in antigen expression levels, the quality of the autologous T cells at baseline, and CAR expression levels. This underlies the critical need to develop on-command mechanisms for remotely calibrating CAR T cell activity levels in patients postinfusion (13, 14).

Chemically induced dimerization (CID) systems, that is, protein–protein interfaces reliant upon the presence of a small chemical compound to bind one another, offer a promising approach for developing inducible ON-switch CARs in which the components necessary for antigen engagement and T cell activation are split among two chains, the receptor (R)-chain and the signaling (S)-chain (15). Ideally, CID-based ON-switches for CARs are nonimmunogenic, will not interfere with cellular function, and the associated small molecule is well tolerated, has favorable pharmacokinetic (PK) properties, and is clinically approved. The first CID-based ON-CAR utilized the FK506 binding protein (FKBP) domain and the T2089L mutant of the FKBP–rapamycin binding domain (FRB*) that heterodimerize in the presence of a rapamycin analog (16). The design has been adapted to include the CID in the ectodomain of ON-CAR chains (13, 17). Such so-called Dimerizing Agent Regulated Immune-Receptor Complex (DARIC) CARs have been translated to the clinic (targeting CD33 for acute myeloid leukemia) but the unfortunate

Author contributions: G.M.P.G.A., S.S., B.E.C., and M.I. designed research; G.M.P.G.A., S.S., E.C., M.T., L.S., M.H., P.R., P.G., and S.G. performed research; G.M.P.G.A., S.S., and M.I. analyzed data; B.E.C. and M.I. directed the study; and G.M.P.G.A., S.S., and M.I. wrote the paper.

Competing interest statement: Provisional intellectual property filing has been filed for iON and iONØ CAR designs with inventors including G.M.P.G.A., B.E.C., SS., and M.I.

This article is a PNAS Direct Submission.

[1]To whom correspondence may be addressed. Email: bruno.correia@epfl.ch or melita.irving@unil.ch.

This article contains supporting information online at https://www.pnas.org/lookup/suppl/doi:10.1073/pnas.2405085121/-/DCSupplemental.

Published October 25, 2024.

recent death of a patient at the study's second dose level put the trial on hold (NCT05105152). The FKBP-FRB CID system has also been used to increase the avidity of 2G CARs comprising weak-binding single-chain variable fragment (scFv) (i.e., AvidCARs) (18). Disadvantages of this CID are that rapamycin can be toxic and immunosuppressive, and although rapalogs are better tolerated they have poor PK properties (19).

More recently, a lipocalin retinol binding protein 4 (hRBP4)-based ON-switch was developed comprising an engineered scaffold having over 500-fold increased binding affinity for hRBP4 in the presence of the orally available drug A1120 (20). In addition, a split ON-switch CAR comprising a ZFP91-1KZF3 hybrid zinc finger mutated to prevent ubiquitination in the R-chain, and CRBNΔ3 in the S-chain endodomain, which dimerize upon administration of lenalidomide, was described (21). Other CIDs have been developed that are plant-based (16, 22) but immunogenicity may be an issue (23). Finally, human antibody based CIDs (e.g., chemical epitope-specific antibodies that can distinguish between Bcl-xL vs. Bcl-xL-ABT-737 complex) have been designed, although not used in the context of split-CARs (24). Overall, few CID-based ON-switch CARs have been developed and new design approaches are warranted.

We previously developed a computationally designed OFF-switch CAR, which we coined the STOP-CAR, controlled by a chemically disruptable heterodimer (CDH). The CDH, encoded in the endodomains of the R- and S-chains, included the B cell lymphoma protein 2 (Bcl-2) family protein Bcl-xL and a selected scaffold protein of human origin engrafted with critical binding residues of the BH3-only protein BIM (14). We showed that in its native state, the STOP-CAR chains associated via the CDH enabling T cell activation in the presence of target antigen. Administration of the disruptive small molecule A-1155463 (which competitively binds Bcl-xL), however, reversibly tuned-down effector function, both in vitro and in vivo.

The STOP-CAR, or more recent degron-based OFF-switch CARs (21, 25) that can be targeted for proteasomal degradation upon administration of lenalidomide, may be favored in the context of known targets like CD19 to prevent CRS. An ON-switch CAR, however, may be preferable for exploring new tumor antigens or coengineering strategies, and an all-in-one ON/OFF-switch CAR enabling faster abrogation of T cell activity could further enhance safety. Here, we have developed a Bcl-2-based ON-switch CAR that can be activated in a dose-dependent manner by venetoclax (or navitoclax) in the presence of a target tumor antigen, as well as proof-of-principle for an all-in-one ON/OFF-switch CAR that is reversibly controlled by venetoclax and lenalidomide.

Results

Bcl-2 Family Proteins Can Be Exploited to Generate Chemically Induced Dimers. We began our study with the intent to exploit Bcl-2 family proteins for generating a CID for an ON-switch CAR. The Bcl-2 family proteins are effectors of canonical mitochondrial apoptosis and they include proapoptotic effectors [e.g., Bcl-2 Associated X-protein (BAX), BCL2 associated agonist of cell death protein (BAD)], proapoptotic BH3-only proteins (e.g., BIM, BID, PUMA), and anti-apoptotic proteins (e.g., Bcl-xL, Bcl-2). Briefly, apoptotic stresses promote the accumulation of BH3-only proteins like BIM which engage and counteract prosurvival proteins including Bcl-xL and Bcl-2, thereby allowing Bax and Bad to form oligomers and permeabilize the mitochondrial membrane (causing cytochrome c release, apoptosome formation, caspase activation, and ultimately cell death) (26). Diverse cancers commonly evade apoptosis by up-regulating anti-apoptotic proteins and as such a variety of BH3 mimetics like venetoclax have been developed (27). Given the role of homo- and hetero-oligomerization among Bcl-2 family proteins in the mitochondrial apoptosis pathway (28), we questioned whether Bcl-2 and Bcl-xL could be triggered by BH3 mimetics to homodimerize and consequently be used as CIDs.

We identified Bcl-xL and the small molecule A-1155463 (henceforth abbreviated A-11) previously used in the context of our STOP-CAR (14), as well as Bcl-2 and venetoclax as promising starting points for developing CIDs. Notably, venetoclax is approved for clinical use. Moreover, although Bcl-2 plays a critical role in immune cell development, response, and homeostasis (29), it was recently demonstrated that venetoclax augments the antitumor efficacy of Immune checkpoint inhibitors (anti-PD-1/PD-L1) and is associated with an increase of PD-1$^+$ effector memory cells. In addition, upon Bcl-2 inhibition, Bcl-xL provides a survival advantage in effector T cells (30).

To investigate possible drug-induced homodimerization of Bcl-2 or Bcl-xL we utilized artificial split transcriptional activator systems (Fig. 1 and *SI Appendix*, Fig. S1) which upon dimerization drive gene expression from a cotransfected reporter plasmid. Briefly, as illustrated in Fig. 1*A*, one copy of Bcl-2 or Bcl-xL is fused to a DNA-binding domain (DBD) which binds upstream of the minimal promoter, and a second copy is linked to an activation domain (AD). For the Gal4-Rel65 reporter system, we observed a substantial fold-increase in reporter expression (firefly luciferase) for Bcl-xL and A-11, as well as for Bcl-2 and venetoclax (Fig. 1*B*). This effect was binding-site-specific because amino acid replacements Y108K and G145A within Bcl-2, and Y101K and G138A within Bcl-xL, which abolish venetoclax and A-11 binding, respectively, abrogated expression of the reporter gene in the presence of the drugs (Fig. 1 *C* and *D*). In addition, the effect was dose-dependent (Fig. 1 *D* and *E*) and small-molecule-specific (Fig. 1*E*). Dimerization of Bcl-2 by venetoclax and of Bcl-xL by A-11 was further validated using two additional reporter systems (*SI Appendix*, Fig. S1).

Bcl-2 Can Be Incorporated into R- and S-Chain Ectodomains to Generate a Venetoclax-Inducible ON-Switch CAR Targeting EpCAM. Given the grand challenge of developing safe and effective next-generation CAR T cells for treating nonhematological solid tumors, as a proof of principle we began by generating a lentiviral vector encoding an inducible (i)ON-CAR targeting epithelial cell adhesion molecule (EpCAM), with truncated Bcl-2 in the ectodomain of both the R- and S-chains (Fig. 2*A*). Briefly, the R-chain included the anti-EpCAM scFv C215 (31) fused to Bcl-2, the hinge and transmembrane (TM) domain of CD8α, and the endodomain of 41BB for costimulation. For the S-chain, we included a c-Myc tag on Bcl-2 which was fused to the hinge and TM domain (TMD) of CD8α, followed by the endodomain of 41BB and of CD3ζ for signal 1 of T cell activation.

We achieved cell-surface expression of the anti-EpCAM iON-CAR by primary human CD4$^+$ and CD8$^+$ T lymphocytes, albeit less efficiently than an equivalent 2G CAR (Fig. 2*B*). We subsequently showed IFNγ production (Fig. 2*C*) and cytotoxicity (Fig. 2*D*) by anti-EpCAM iON-CAR T cells upon coculture with target tumor cells, but only in the presence of venetoclax. In contrast, there was no impact of venetoclax at the concentrations used on function of the 2G-CAR T cells. Based on the favorable and controllable in vitro activity of anti-EpCAM iON-CAR T cells, we next tested them in vivo (Fig. 2*E*). We demonstrated control of subcutaneous PC3-PIP tumors (which naturally express EpCAM) by the iON-CAR T cells only upon coadministration of venetoclax. The

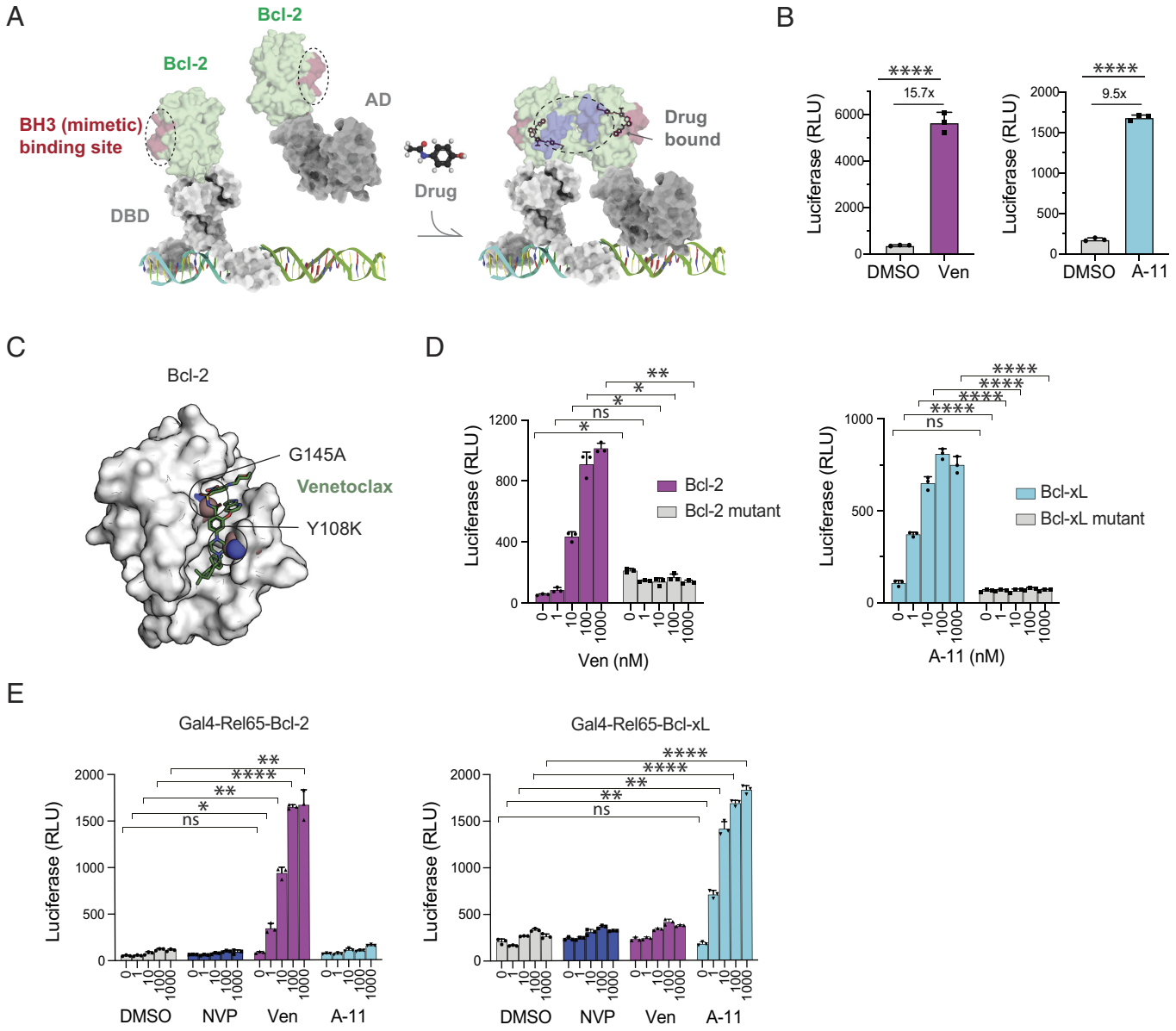

Fig. 1. Demonstration that Bcl-2 and venetoclax as well as Bcl-xL and A-11 constitute chemically induced dimers. (*A*) Schematic of mammalian two-hybrid system based on split chimeric transcription factors (TF) that trigger reporter gene expression upon dimerization of the DBD and the AD. (*B*) Gene expression (luciferase) at 24 h from a reporter plasmid encoding UAS-GAL4 response elements for a two-hybrid system comprising GAL4 (galactose-responsive TF) and Rel65 (NF-kB p65) fused to Bcl-2 (in purple) or Bcl-xL (in light blue) ±100 nM venetoclax (Ven) or A-11 (A-1155463), respectively (or DMSO). (*C*) Structure of Bcl-2 (PDB id: 6o0k) with mutations Y108K and G145A that abrogate venetoclax (in green) binding. Bcl-xL with mutations Y101K and G138A does not bind A-11 (not shown). (*D*) Reporter gene expression (luciferase) at 24 h from a reporter plasmid encoding UAS-GAL4 response elements for two-hybrid systems comprising GAL4 and Rel65 (NF-kB p65) fused to Bcl-2 (purple) or Bcl-2 mutant (in gray; Y108K, G145A) or Bcl-xL (light blue) or Bcl-xL mutant (in gray; Y101K, G138A) ±increasing concentrations of venetoclax (Ven) or A-1155463, respectively. (*E*) Gene expression (luciferase) at 24 h from a reporter plasmid encoding UAS-GAL4 response elements for two-hybrid systems comprising GAL4 and Rel65 fused to Bcl-2 (*Left*) or Bcl-xL (*Right*) ±Increasing concentrations of DMSO, NVP-CGM097 (nonspecific molecule), venetoclax (Ven), or A-1155463. (ns = nonsignificant $*P < 0.05$ $**P < 0.01$. Ven = venetoclax; A-11 = small molecule A-1155463; SEAP = secreted alkaline phosphatase. All experiments performed in HEK-293T cells.

equivalent 2G-CAR T cells, however, controlled tumors regardless of the presence or absence of venetoclax.

Encouraged by these data and to demonstrate the universality of the system, we next generated a CD19-specific iON-CAR with the commonly used scFv FMC63 (32) (*SI Appendix*, Fig. S2*A*). We demonstrated cell-surface expression of the iON-CAR as well as an equivalent 2G CAR by both $CD4^+$ and $CD8^+$ T lymphocytes (*SI Appendix*, Fig. S2 *B* and *C*). In an IncuCyte assay we observed cytotoxicity of the PC3-PIP cell line engineered to express CD19 (PC3-PIP-CD19) in the presence of venetoclax (*SI Appendix*, Fig. S2*D*). In coculture assays with these target cells we similarly demonstrated IFNγ production (*SI Appendix*, Fig. S2*E*) by the iON-CAR T cells only if venetoclax was present. In a FACS-based cytotoxicity assay of the $CD19^+$ liquid tumor cell lines BV173 (acute lymphoblastic leukemia) and Daudi (B-lymphoblast) (*SI Appendix*, Fig. S2 *F* and *G*), however, we found that while newly generated anti-CD19 iON-CAR T cells can efficiently eliminate target cells upon addition of venetoclax, in cocultures of 12 h or more there was significant killing even in the absence of venetoclax (*SI Appendix*, Fig. S2*H*). In contrast, there was no killing under these conditions of CD19 knockout BV173 cells (*SI Appendix*, Fig. S2*I*) (33). Hence we conclude that although this iON-CAR is specific for $CD19^+$ target cells, over time the scFv FMC63 drives clustering of the R- and S-chains in the absence of venetoclax (i.e., it behaves like a 2G CAR) and it is not suitable for our iON-switch CAR design.

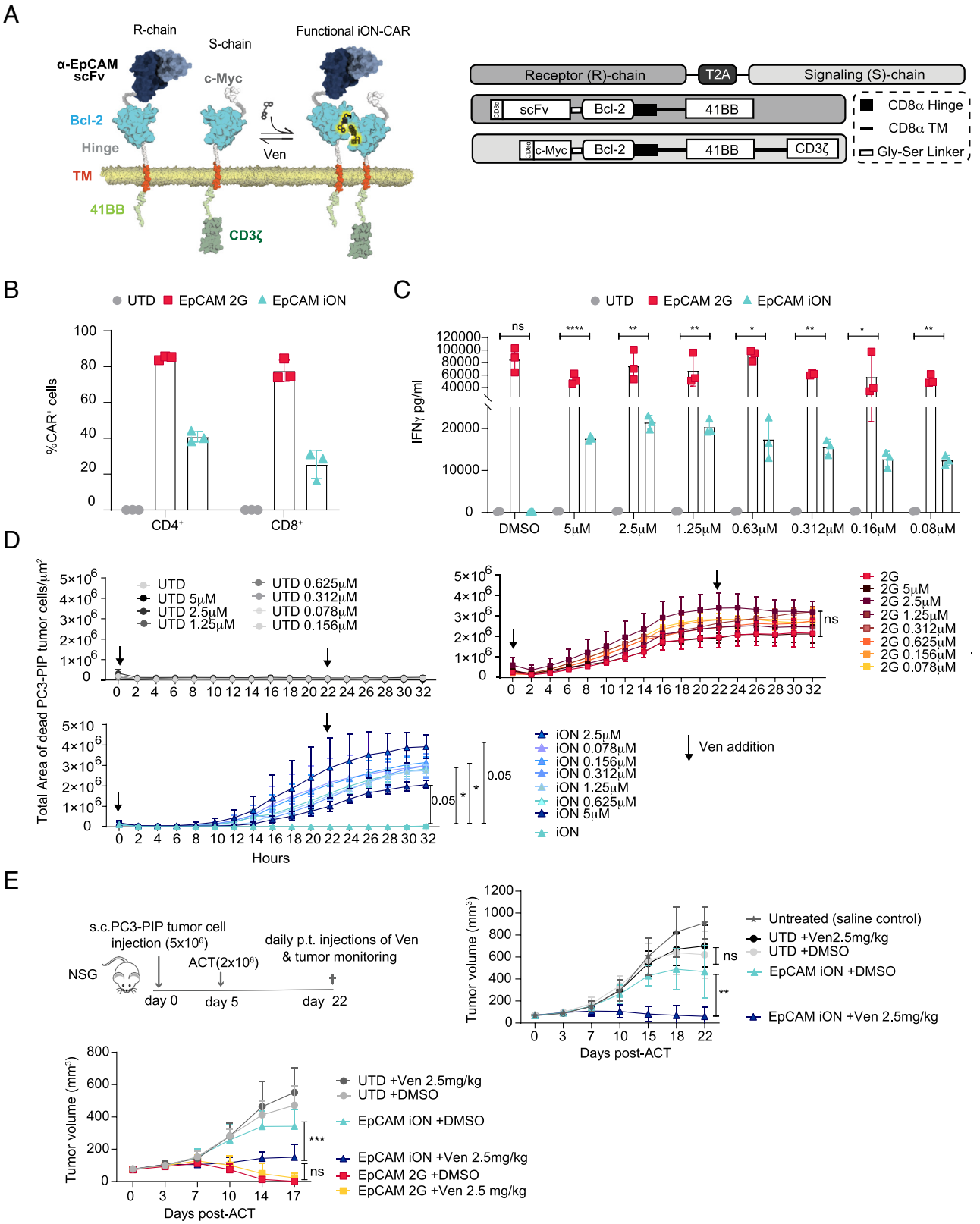

Fig. 2. Bcl-2-based iON-CAR T cells targeting EpCAM are functional in vitro and in vivo in the presence of venetoclax. (*A*) Schematic (*Left*) and lentiviral vector design (*Right*) of iON-CAR targeting EpCAM. (*B*) Evaluation of 2G- and iON-CAR expression by cell-surface staining in the presence of 5 μM venetoclax (after 12 h incubation) by anti-Fab staining (n = 3 HD). (*C*) Interferon-gamma (IFNγ) production by CAR T cells in coculture with EpCAM$^+$ PC3-PIP tumor cells ± venetoclax (range from 5 to 0.078 μM; effector to target ratio of 1:1). A two-way ANOVA with the post hoc Tukey test was used for statistical analysis, comparing all groups; ns = nonsignificant *$P < 0.05$ **$P < 0.01$ ****$P < 0.0001$. Comparison reported on graph for iON versus UTD under all conditions. (*D*) IncuCyte cytotoxicity assay of EpCAM$^+$ PC3-PIP tumor cells by the different CAR T cells ± venetoclax (from 5 to 0.078 μM) over time (n = 3 HD). Target cell killing is reported as total area of dead cells, as measured by Cytotoxic Red reagent uptake (red area per μm^2). A two-way ANOVA with the post hoc Tukey test was used for statistical analysis, comparing iON+DMSO vs. iON+venetoclax; ****$P < 0.0001$. (*E*, *Top Left*) schematic of in vivo studies. (*Top Right* and *Bottom Left*) PC3-PIP tumor control by UTD and CAR T cells generated from two different donors ± venetoclax (2.5 mg/kg) over days. Values are the mean ± SEM of n = 7 mice per group. A two-way ANOVA with the post hoc Tukey test was used for statistical analysis, comparing all T cell groups at day 17 or 22 (two independent replicates have been performed). R-chain = receptor chain; S-chain = signaling chain; TM = transmembrane; UTD = untransduced; HD = T cells from healthy donor; TM = transmembrane; Ven = venetoclax.

Anti-Prostate-Specific Membrane Antigen (PSMA) iON-CAR T Cells Are Functional In Vitro and In Vivo in the Presence of Venetoclax and Target Tumor Cells. To further validate our Bcl-2 and venetoclax-based ON-switch in engineered T cells, we subsequently built an iON-CAR targeting the PSMA (Fig. 3*A*) with scFv J591 (34) which we previously used in our STOP-CAR and 2G CAR designs (14, 35). We demonstrated cell-surface expression of the anti-PSMA iON-CAR and corresponding 2G CAR in both $CD4^+$ and $CD8^+$ T lymphocytes, typically at lower efficiency for the latter (Fig. 3 *B* and *C*).

We and others have shown that the anti-apoptotic protein Bcl-2 is up-regulated in activated CAR T cells (8), and enforced Bcl-2 overexpression has long been known to augment survival of tumor-specific T cells (36). Thus, we next questioned if exposure to venetoclax induces apoptosis in activated CAR T cells. We set up cocultures of UTD, 2G, and iON-CAR T cells with target tumor cells ± venetoclax and 24 h later stained for markers of apoptosis, AnnexinV and 7AAD (Fig. 3*D*). At 5 μM venetoclax, the highest concentration not toxic to the target PC3-PIP tumor cells, we observed a significant increase in the percentage of T cells undergoing late apoptosis in all experimental groups. At 2.5 μM venetoclax, however, there was not a significant increase in late apoptosis of the activated CAR T cells. In the absence of target cells, venetoclax augmented both early and late markers of apoptosis in both UTD and CAR T cells. This may in part be due to the fact that the CAR T cells are not activated (i.e., Bcl-2 levels are lower in the cells) and there are no tumor cells in the culture wells that can also uptake the drug (*SI Appendix*, Fig. S3*A*).

Next, we evaluated the effector function of PSMA-targeted iON-CAR vs. 2G-CAR T cells ± venetoclax. The iON-CAR T cells were cytotoxic (Fig. 3*E* and *SI Appendix*, Fig. S3 *B* and *C*) and produced IFNγ (Fig. 3*F* and *SI Appendix*, Fig. S3*D*) upon coculture with target cells in the presence of venetoclax, demonstrating functionality of the iON-switch. In the absence of target antigen the iON-CAR T cells were inactive ± venetoclax (*SI Appendix*, Fig. S3 *E* and *F*). We further sought to evaluate how quickly iON-CAR T cells lose function upon venetoclax withdrawal. A 50% drop in IFNγ production was observed at 24 h and complete abrogation by 48 h after venetoclax removal from coculture with target tumor cells (Fig. 3*G*). Importantly, after a short period of rest iON-CAR T cells can be reactivated upon tumor antigen exposure in the presence of venetoclax (Fig. 3*H*). For some iON-CAR T cell donors leakiness was observed as IFNγ production or target cell killing were observed in the absence of venetoclax, but levels were typically very low. Notably, the iON-CAR T cells could also be activated upon target cell exposure in the presence of the BH3 mimetic Navitoclax (*SI Appendix*, Fig. S4).

Finally, we tested the iON-CAR T cells vs. equivalent 2G-CAR T cells in vivo. We demonstrated robust control of subcutaneous PC3-PIP tumors by anti-PSMA iON-CAR T cells upon coadministration of venetoclax, with the same efficacy as equivalent 2G-CAR T cells (Fig. 3*I*). In the absence of venetoclax the iON-CAR T cells did not control tumors, although there was some impact on tumor outgrowth as compared to control mice. In addition, venetoclax on its own or coadministered with UTD T cells had no impact on tumor growth, and venetoclax did not influence tumor control by 2G-CAR T cells (Fig. 3*I* and *SI Appendix*, Fig. S5). Notably, in a long-term in vivo study, we demonstrated complete control of tumors by iON-CAR T cells in the presence of venetoclax up until day 50, the study endpoint (*SI Appendix*, Fig. S5*C*). Thus, both the in vitro and in vivo function of the anti-PSMA iON-CAR T cells is reliant upon the presence of venetoclax and the engagement of target antigen.

Degrons Encoded in the S- and R-Chain Endodomains Enable Reversible Lenalidomide-Mediated CAR Downregulation. As described above, by 48 h postvenetoclax withdrawal we found that iON-CAR T cells were no longer responsive to target tumor cells (Fig. 3*G*) and we questioned if we could increase the rate of inactivation of the iON-CAR. Taking inspiration from recent studies (25), we encoded an optimized degron sequence (21) at the C terminus of both the S- and R-chains to generate an all-in-one ON/OFF-switch CAR which we coined the iONØ-CAR prototype (iONØp-CAR) (*SI Appendix*, Fig. S6*A*). Briefly, a degron is a specific sequence within a protein that targets it for degradation within the cell, and degrons (or optimized super-degrons) can be fused to a protein of interest such as a CAR (21) to mark it for proteasomal degradation upon administration of thalidomide or one of its derivatives (e.g., lenalidomide and pomalidomide) which act by targeting the degron-tagged protein to an E3 ubiquitin ligase (37).

In the presence lenalidomide we observed intracellular 2G and iON-CAR expression by anti-Fab staining but the iONØp-CAR was not detected, indicative of successful proteasomal degradation (*SI Appendix*, Fig. S6*B*). We further demonstrated abrogation of IFNγ production and target cell killing by iONØp-CAR T cells in the presence of venetoclax plus lenalidomide but the 2G- and iON-CAR T cells remained fully functional under these same conditions (*SI Appendix*, Fig. S6 *C* and *D*). Finally, we sought to determine how quickly the iONØp-CAR could be down-regulated in T cells. In a kinetic assay, we observed that between 4 to 6 h postexposure to lenalidomide the iONØp-CAR was no longer detectable (*SI Appendix*, Fig. S6*E*).

Subsequently, in an attempt to improve expression levels of the iONØ-CARp, we moved the degron sequence from the C terminus of the S-chain to between the 41BB and CD3ζ endodomains (Fig. 4*A*). This design, which we refer to as iONØ-CAR, did not impact fold-expansion of transduced T cells (Fig. 4*B*), and it improved transduction efficiency in both $CD8^+$ and $CD4^+$ T cells to levels similar to the iON-CAR (Fig. 4*C*). Along with higher transduction efficiency than the original iONØp-CAR, it was also expressed at higher levels per cell (higher mean fluorescence intensity; MFI, *SI Appendix*, Fig. S6*F*). There were no significant differences in the upregulation of apoptotic markers in iONØ-CAR T cells following overnight culture with venetoclax as compared to UTD T cells (*SI Appendix*, Fig. S6*G*).

In functional assays, we demonstrated both IFNγ production (Fig. 4*D*) and cytotoxicity (Fig. 4*E*) of iONØ-CAR T cells in cocultures with $PSMA^+$ target tumor cells in the presence of venetoclax. However, coadministration of lenalidomide with venetoclax rendered the iONØ-CAR T cells inactive (Fig. 4 *D* and *E*). Importantly, in a tumor cell rechallenge assay, we demonstrated that iONØ-CAR T cells regain effector function (as measured by IFNγ production) in the presence of venetoclax and target tumor cells post lenalidomide exposure and a resting period (Fig. 4*F*). Moreover, iONØ-CAR T cells can respond to a second challenge of tumor cells in the presence of venetoclax, but not if lenalidomide is also added to the coculture (Fig. 4*F*). In other words, iONØ-CAR T cells can be reversibly switched ON and OFF and can be serially activated in vitro. We also found that lenalidomide could abrogate IFNγ production by iONØ-CAR T (activated by target tumor cells in the presence of venetoclax) within 24 h in coculture assays (Fig. 4*G*). Finally, we demonstrated that iONØ-CAR T cells can fully control target tumors upon adoptive cell transfer (ACT) in the presence of venetoclax (*SI Appendix*, Fig. S6*H*). In future studies, we plan to explore the possibility of dynamically tuning up and down the activity levels of the iONØ-CAR T cells in vivo.

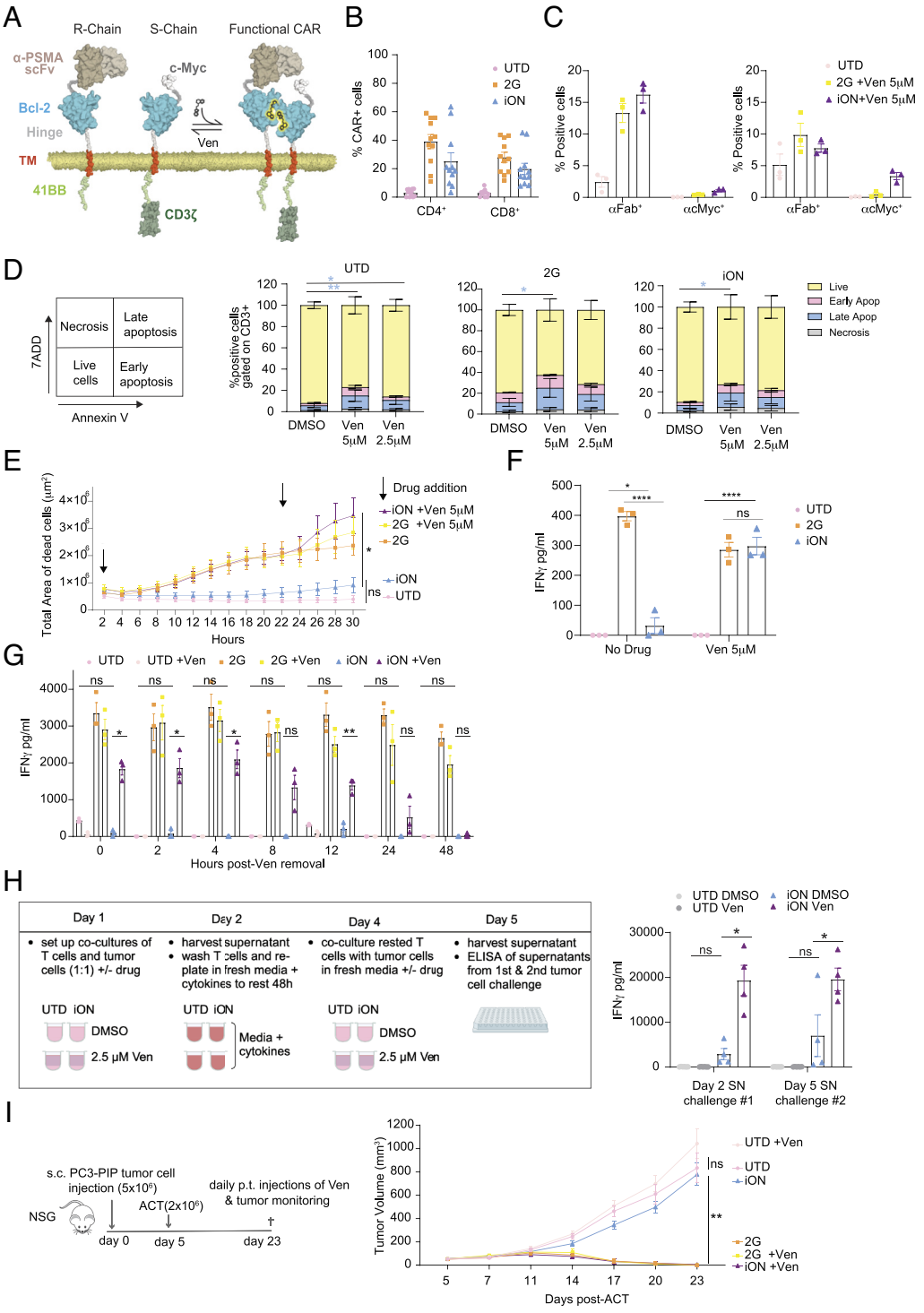

Fig. 3. Bcl-2-based iON-CAR T cells targeting PSMA are functional both in vitro and in vivo in the presence of venetoclax. (*A*) Schematic of split iON-CAR targeting PSMA. (*B*) Evaluation of 2G- and iON-CAR expression by intracellular anti-Fab staining (n = 12 HD). (*C*) $CD4^+$ (*Left*) and $CD8^+$ (*Right*) T cell-surface staining in the presence of venetoclax (after 12 h incubation) of 2G CAR by anti-Fab staining (n = 3 HD) and of iON CAR by anti-Fab (R-chain) and anti-cMyc staining (S-chain) (n = 3 HD). (*D*) Evaluation of Annexin V/7ADD induced expression after 24 h coculture of T cells with tumor cells (1:1 E:T Ratio) in presence of DMSO or 2.5 μM venetoclax. (n = 6 pooled from two independent experiments). (*E*) IncuCyte cytotoxicity assay of $PSMA^+$ PC3-PIP tumor cells by the different CAR T cells ± venetoclax over time (n = 6 HD pooled from two independent experiments). Target cell killing is reported as total area of dead cells, as measured by Cytotoxic Red reagent uptake (red area per μm^2). A two-way ANOVA with the post hoc Tukey test was used for statistical analysis, comparing all groups; $^*P < 0.05$. (*F*) IFNγ production by CAR T cells and UTD T cells upon coculture with PC3-PIP tumor cells ± venetoclax (n = 3 HD), two independent replicates. A two-way ANOVA with the post hoc Tukey test was used for statistical analysis, comparing iON vs. 2G CAR and iON vs. UTD; $^{****}P < 0.0001$: ns = nonsignificant. (*G*) IFNγ production by UTD and CAR T cells (n = 3 HD) upon coculture with PC3-PIP tumor cells (effector to target ratio of 1:1) at various hours post venetoclax removal (after 12 h preincubation or not). A two-way ANOVA with the post hoc Tukey test was used for statistical analysis, comparing all groups; $^*P < 0.05$. $^{**}P < 0.005$. (*H*, *Left*) schematic of the experiment; (*Right*) IFNγ production by CAR T cells and UTD T cells upon coculture with PC3-PIP tumor cells ± venetoclax, washed and rested for 48 h and after a second coculture with tumor cells (n = 4 HD), two pooled independent experiments. (*I*, *Left*) schematic of in vivo study. (*Right*) PC3-PIP tumor growth or control by UTD vs. CAR T cells ± venetoclax (2.5 mg/kg) over days. Values are the mean ± SEM of n = 7 mice per group. A two-way ANOVA with the post hoc Tukey test was used for statistical analysis with significance indicated considering all T cell groups at day 23 (four independent studies were conducted). Reported on the graph statistic for iON, DMSO vs. iON +Ven. iON, DMSO vs. UTD. R-chain = receptor chain; S-chain = signaling chain; TM = transmembrane; UTD = untransduced; HD = T cells from healthy donors; SN = supernatant.

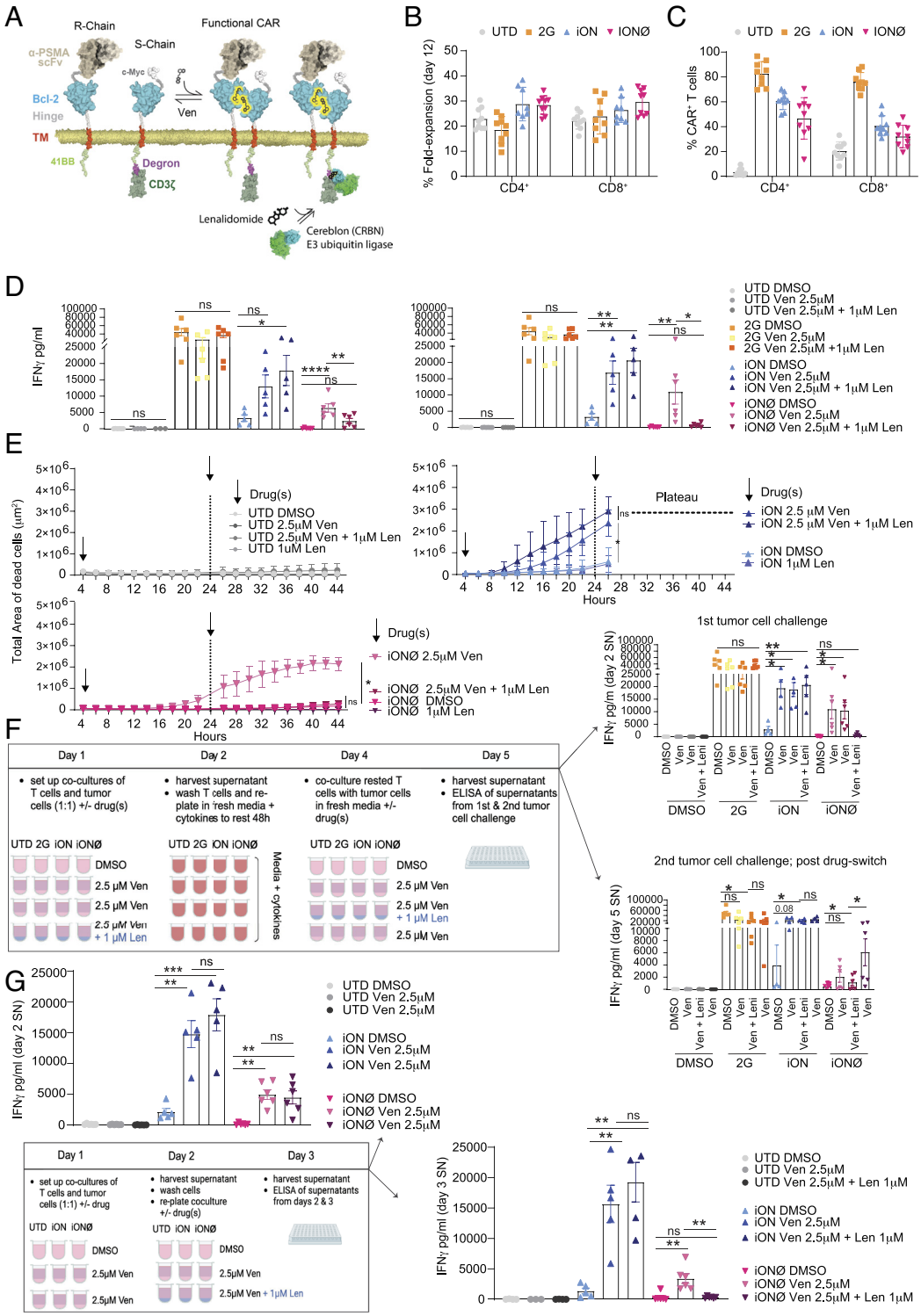

Fig. 4. All-in-one ON/OFF-switch CAR T cells targeting PSMA can be reversibly controlled with venetoclax and lenalidomide. (*A*) Schematic of iONØ-CAR targeting PSMA that is switched into active mode in the presence of venetoclax and can be down-regulated via the degron encoded in the S-chain in the presence of lenalidomide. (*B*) Fold increase of iONØ-CAR at day 12 from transduction for $CD4^+$ and $CD8^+$ T cells (n = 9 HD). (*C*) Percentage of surface CAR-expressing T cells by αFab CAR staining after overnight exposure to venetoclax (n = 9 HD). (*D*) IFNγ production by CAR T cells upon coculture with PC3-PIP cells ± venetoclax and lenalidomide at concentrations as shown. Values are the mean ± SEM for n = 5 to 6 HD (two pooled independent experiments). One-way ANOVA test comparing each single experimental group per type of treatment has been applied to determine statistical significance. (*E*) IncuCyte cytotoxicity assays of PC3-PIP cells and UTD or CAR T cells ± venetoclax (2.5 μM) and ± lenalidomide (1 μM) as shown. Target cell killing is reported as the total area of dead cells, as measured by Cytotoxic Red reagent uptake (red area per μm^2). Values are the mean ± SEM of n = 3 HD. Two independent replicates were performed. Two-way ANOVA test comparing all experimental groups has been applied to determine statistical significance. (*F*, *Left*) schematic of the experiment. (*Right*) IFNγ production before (*Top*) and after (*Bottom*) a resting time of 48 h by CAR T cells upon coculture with PC3-PIP cells ± venetoclax and lenalidomide is reported. Values are the mean ± SEM for n = 5 to 6 HD (two pooled independent experiments). One-way ANOVA test comparing each single experimental group per type of treatment has been applied to determine statistical significance. (*G*, *Bottom Left*) schematic of the experiment. IFNγ production of CAR T cells upon coculture with PC3-PIP cells ± venetoclax and lenalidomide is reported before (*Top Right*) and after (*Bottom Right*) activation by target cells. Values are the mean ± SEM for n = 4 to 6 HD (two pooled independent experiments). One-way ANOVA test comparing each single experimental group per type of treatment has been applied to determine statistical significance. UTD = untransduced; HD = T cells from healthy donors; SN = supernatant.

Discussion

Chemically inducible proximity systems are widely utilized in synthetic biology to generate artificially controlled biological circuitries (38). Many of these systems can serve as the basis for important translational applications, such as introducing safety switches in cell-based therapies (14). However, the array of responsive proteins remains restricted due to limited chemical space and potential concerns with immunogenicity of the components. In our study, we demonstrated that human proteins Bcl-2 and Bcl-xL can be repurposed into CIDs with the BH3 mimetics venetoclax (or navitoclax) and A-1155463, respectively. Exploiting the dimerizing capacity of Bcl-2 in the presence of venetoclax, we developed a split iON-switch CAR comprising an R-chain (bearing the scFv) and an S-chain (encoding the CD3ζ endodomain), thereby dissociating tumor antigen binding from T cell activation. Following the previous design evolution of FKBP-based ON-CARs (i.e., DARIC), we incorporated Bcl-2 into the ectodomain of the two chains under the assumption that lower concentrations of venetoclax could be used to trigger their association (16, 17).

It should be noted that along with CID and disruptive strategies (i.e., CID and CDH), innovative protease-based designs have also been used to integrate switches into CARs. For example, for the VIPER (Versatile ProtEase Regulatable) ON-switch CAR the nonstructural protein 3 (NS3; a proteolytic protein in the hepatitis C virus lifecycle) is encoded in the endodomain and flanked by cleavage sites. As such, in the absence of grazoprevir (a clinically approved small molecule that blocks NS3) the CAR is fragmented by cis-proteolysis but in its presence, the CAR remains assembled and responsive to target antigen. A second protease-based platform, the so-called Signal Neutralization by an Inhibitable Protease CAR (39), also integrates NS3-based proteolysis to create an ON-switch, in both a cis format (like the VIPER) and a trans format (i.e., NS3 is encoded on a second chain and can cleave the CAR in the absence of grazoprevir) (39). While these designs are reported highly functional and minimally leaky, an important risk is immunogenicity of NS3 and consequent depletion of the engineered T cells as the immune system regenerates in lymphodepleted patients.

In our study, using a single lentiviral vector encoding both the R- and S-chains, we successfully expressed our iON-CAR on the surface of primary human T cells. We demonstrated that with a suitable scFv, iON-CAR T cells are responsive to target tumor cells in the presence of venetoclax (or navitoclax). We developed iON-CARs for targeting both EpCAM and PSMA and found that post venetoclax withdrawal, they lost their ability to respond to target tumor cells within 48 h (as evaluated by abrogation in IFNγ production). A low level of iON-CAR leakiness was observed for some T cell donors (e.g., low IFNγ production in the absence of venetoclax) but we argue that the purpose of the remote-control design is to tune up or tune down activity levels. To achieve full shut-down, a suicide switch could be further coengineered into the T cells (3). However, while anti-CD19 iON-CAR T cells were only reactive against $CD19^+$ target cells, in longer coculture assays they behaved like 2G CAR-T cells in that venetoclax was no longer required for their activation. Presumably, this is a consequence of properties of the scFv (FMC63) (32) used and it shows that not all scFv are suitable for this iON-switch design, as not all scFv optimal for classic 2G CARs (40). Other components of the CAR such as the linker and TMD could also be modified in an attempt to mitigate R- and S-chain association in the absence of venetoclax.

We have further presented proof-of-principle for an all-in-one ON/OFF-switch CAR, coined the iONØ-CAR, that is turned on with one molecule (venetoclax) and down-regulated by a second drug (lenalidomide) within 4 to 6 h. Notably, both of these drugs are approved for clinical use in the context of cancer treatment, are tolerated by patients, and do not negatively impact the function of T cells at doses used in our study (30, 37). We improved the cell surface expression (both transduction efficiency and MFI) of the iONØ-CAR by relocating the degron sequence from the C terminus of the S-chain to between the endodomains of 41BB and CD3ζ. Importantly, we showed that iONØ-CAR T cells can be rendered nonresponsive to target tumor cells within 24 h in the presence of lenalidomide. Moreover, iONØ-CAR T cells fully regain their function post lenalidomide withdrawal in the presence of target tumor cells and venetoclax.

Future studies should include determining how the R- and S-chains of the iON-CAR and iONØ-CAR associate in the cell membrane upon venetoclax administration as both hetero- and homodimerization are possible. In addition, the kinetics of these remote-control CAR T-cells in vivo (i.e., how quickly/efficiently they can be reversibly tuned up or down), as well as their ability to alleviate exhaustion upon transient rest (41) and to abrogate toxicity should be studied. Although toxicity to the engineered lymphocytes is not anticipated in patients receiving venetoclax at doses to trigger the CARs, Lee et al. demonstrated that CAR-T cells can be coengineered to express mutated Bcl-2 (F104L) not recognized by venetoclax for resistance and enhanced function, and this could also be incorporated into our strategy (42). ON- and ON/OFF-switch CAR T cells also offer greater security in coengineering of immunomodulatory molecules under an activation inducible promoter so that secretion is confined to the tumor microenvironment (3, 7) and production will cease upon venetoclax withdrawal or/and lenalidomide administration. Overall, our Bcl-2-based iON-CAR and iONØ-CAR offer important opportunities for developing safe and effective next-generation T cell therapies against cancer for clinical translation.

Materials and Methods

Bcl-2 and Bcl-xL Constructs. For Bcl-2 and Bcl-xL we used modified sequences derived from PDB ID 4lvt and 4qvf, respectively, including truncation of the TMD to the outer mitochondrial membrane (amino acids 208 to 239 and 210 to 239, respectively), and a deletion of the flexible loop domain between the first and second protein helices (amino acids 31 to 70 for both).

Compounds. Venetoclax (>99.9%, Chemietek CT-A199), A1155463 (99.5%, Chemietek CT-A115), and NVP-CGM097 (100% optically pure, Chemitek CT-CGM097) were dissolved in Dimethylsulfoxide (DMSO) as 10 mM stocks, which were aliquoted and stored at −20 °C until use.

HEK293T Cell Culture and Transfection. HEK293T cells were maintained in Dulbecco's Modified Eagle Medium with 10% fetal bovine serum (FBS) (Gibco) and Pen/Strep (Thermo Fisher). Cells were split every two days at approximately 80% confluence. HEK293T cells were seeded 24 h before transfection with the lipofectamine 3000 kit (Thermo Fisher). For drug induction experiments, the small molecules were added 12 h posttransfection and incubated with cells for 24 h before the reporter detection assay.

Reporter Constructs. To investigate drug-induced homodimerization of Bcl-2 or Bcl-xL, 3 reporter systems were built. For the first reporter system, Gal4 [galactose-responsive transcription factor (TF) GAL4] and Rel65 (TF p65/nuclear factor NF-kappa-B p65) were fused either to Bcl-2 or Bcl-xL. The formation of Gal4-Bcl2:Bcl2-p65 dimers (upon administration of venetoclax), for example, triggers reporter gene expression from a reporter plasmid containing UAS-Gal4 response elements. To test for drug specificity, the effects of a panel of Bcl-2 family inhibitors and a nonrelated mdm2 inhibitor were tested on the Gal4/UAS split TF system. For the second reporter system, Bcl-2 or Bcl-xL were fused to TetR (repressor of the tetracycline resistance element) and VP16 (Herpes simplex virus protein vmw65) which together can drive

drug-dependent reporter gene expression from reporter plasmids containing Tet response elements. For the third reporter system, Bcl2 or Bcl-xL were fused to the coat protein of the RNA bacteriophage MS2 (MCP) and the transcriptional activator VPR. The MCP fusion protein binds sgRNAs with a modified stem–loop structure and colocalizes with a dead (d)Cas9 bound to genomic regions of choice. This system was tested with guide Ribonucleic acid (gRNAs) specific for the insulin promoter and confirmed the function with a reporter plasmid containing the respective insulin promoter sequences.

Reporter Detection. Firefly luciferase activity was measured using the cell lysate. Briefly, the cells were lysed in 100 μL buffer containing 32 mM Tris pH 7.9, 10 mM MgCl2, 1.25% Triton X-100, 18.75% glycerol, and 1 mM Dithiothreitol. 50 μL lysate samples were transferred to a 96-well plate with white background (Sigma, # CLS3912). 50 μL of lysis buffer supplemented with 1 μg/mL luciferin (Sigma, #L-6882) and 2 mM Adenosine triphosphate (Sigma, #A3377) were added to each well immediately before reading the luminescence signal on a Tecan Infinite 500 plate reader. Secreted alkaline phosphatase (SEAP) activity (U/L) in cell culture supernatants was quantified by kinetic measurements at 405 nm (1 min/measurement for 30 cycles) of absorbance increase due to phosphatase-mediated hydrolysis of para-nitrophenyl phosphate (pNPP). 4 to 80 μL of supernatant was adjusted with water to a final volume of 80 μL, heat-inactivated (30 min at 65 °C), and mixed in a 96-well plate with 100 μL of 2× SEAP buffer (20 mM homoarginine (FluorochemChemie), 1 mM MgCl2, 21% (v/v) diethanolamine (Sigma Aldrich, D8885), pH 9.8) and 20 μL of substrate solution containing 20 mM pNPP (Sigma Aldrich, 71768). Split luciferase activity was measured using the NanoGlo assay kit (Promega, N1110).

Drug Knockout Mutations. Amino acid replacements G138A and Y101K lining the BH3-binding pocket have been reported to inhibit Bcl-xL binding to Bax (40). By sequence alignment, we determined that these residues correspond to G142 and Y105 of the BH3-binding pocket of BCL2. These amino acid replacements were introduced to confer resistance to small molecule BH3 mimetics.

Cell Lines. Prostate carcinoma cell lines targeted in this study included PC3-PIP (PSMAhi), PC3 (PSMA-), PC3-PIP-CD19+ (PSMAhiCD19hi). Additional tumor cell targets included, BV173, BV173-CD19 KO, and Daudi. Human embryonic kidney 293T cells (HEK-293T) were used for lentivirus production. All cell lines were cultured in Roswell Park Memorial Institute Medium (RPMI)-1640 medium, supplemented with 10% heat-inactivated FBS, 2 mmol/L L-glutamine, 100 μg/mL penicillin, and 100 U/mL streptomycin, maintained at 37 °C in a 5% CO_2 atmosphere (Invitrogen, Life Technologies). The HEK-293T cell line was purchased from the American Type Culture Collection. PC3-PIP and PC3 cells were kindly provided by A. Rosato (University of Padua, Padova). The PC3-PIP-CD19$^+$ cell line was generated and shared by Y. Muller (University of Lausanne), and BV173, Daudi, and BV173-CD19 KO lines were provided by C. Arber (Ludwig Institute for Cancer Research, University of Lausanne and CHUV hospital).

iON-CAR and iONØ-CAR Constructs. The iON-CAR constructs comprising R- and S-chains were synthesized as gene strings (GeneArt, Thermo Fischer Scientific) and cloned into a third-generation self-inactivating lentiviral vector, pELNS, under the control of the EF-1α promoter. The R-chain included a CD8α leader sequence, scFv, truncated Bcl-2, CD8α hinge, CD8 TMD, and 41BB extracellular domain (ED). The S-chain included a CD8α leader sequence, c-Myc, truncated Bcl-2, CD8α hinge, CD8 TMD, 41BB ED, and CD3ζ ED. The scFv derived from monoclonal antibodies C215 (anti-EpCAM) (31), FMC63 (anti-CD19) (32), and J591 (anti-PSMA) (34) were used in the R-chains. For the iONØ-CAR constructions, a super-degron sequence developed by Jan et al. (21) was encoded either at the C terminus of both chains (for the iONØp), or at the C terminus of the R-chain and between 41BB and the CD3ζ endodomains on the S-chain (for the iONØ-CAR).

Recombinant Lentivirus Production. High-titer replication-defective lentivirus was produced and concentrated by ultracentrifugation for primary T cell transduction. Briefly, 24 h before transfection, 10×10^6 HEK293T cells were seeded in 30 mL medium in a T-150 tissue culture flask. All plasmid DNA was purified using the Endo-free Maxiprep kit (Invitrogen, Life Technologies). HEK293T cells were transfected with 7 μg pVSV-G (VSV glycoprotein expression plasmid), 18 μg of R874 (Rev and Gag/Pol expression plasmid), and 15 μg of pELNS transgene plasmid, using a mix of Turbofect (Thermo Fisher Scientific AG) and Optimem medium (Invitrogen, Life Technologies, 180 μL of Turbofect for 3 mL of Optimem). Virus supernatant was collected 48 h after transfection and viral particles were concentrated by ultracentrifugation for 2 h at 24,000 g, resuspended in 400 μL complete RPMI-1640 medium, and immediately snap frozen on dry ice.

Primary Human T Cell Transduction. Primary human T cells were isolated from the peripheral blood mononuclear cells (PBMCs) of healthy donors (HD; prepared as buffycoats) collected with informed consent. All gene modifications to T cells were made with ethics approval to the laboratory from the Canton of Vaud (Federal Office for the Environment; ECOGEN, A-130579-1). PBMCs were enriched by Lymphoprep (Axonlab) separation solution with a standard protocol of centrifugation. CD4$^+$ and CD8$^+$ T cells were isolated using a magnetic bead-based negative selection kit following the manufacturer's recommendations (easySEP, Stem Cell technology) and cultured at a 1:1 ratio in RPMI-1640 with Glutamax, supplemented with 10% heat-inactivated FBS, 100 U/mL penicillin and 100 μg/mL streptomycin sulfate and stimulated with anti-CD3/anti-CD28-beads (Invitrogen, Life Technologies) at a ratio of 1:2 T cells to beads. T cells were transduced at 18 to 22 h after activation with lentivirus and human recombinant IL-2 (h-IL-2; Peprotech) was replenished every other day for a concentration of 50 IU/mL until 5 d after stimulation. At this time point, the magnetic beads were removed, and human-IL-7 and IL-15 (Miltenyi Biotec GmbH) were added to the cultures at 10 ng mL/1. For expansion, a cell density of 0.5 to 1×10^6 cells/mL was maintained. Before all functional assays, the engineered T cells were adjusted for equivalent transgene expression and rested (no cytokine addition for 48 h).

Cytokine Release Assays. Cytokine release assays were performed by duplicate coculture of T cells with target cells (5×10^4 of each) in a final volume of 200 μL of RPMI medium per well in 96-well round-bottom plates. Coculture supernatants were collected after 24 h and tested for the IFNγ levels detected by enzyme-linked immunosorbent assay following the manufacturer's protocol (BioLegend). Reported values represent the mean of cytokine production by CAR-engineered T cells derived from HDs ± SEM.

Serial Coculture Assays. For serial coculture assays, 1×10^5 target tumor cells were seeded in 96-well U-bottom plates (Costar, Vitaris). Rested T cells, normalized for equal CAR expression, were added at 1×10^5 per well and then incubated at 37 °C in the presence or absence of drug. After 24 h, supernatants were collected and the T cells were washed and re-exposed to new tumor targets at a 1:1 ratio, either after a 48 h rest period or immediately following the first coculture.

Cytotoxicity Assays. Target cell killing was evaluated with the IncuCyte Instrument (Essen Bioscience). Briefly, 1.25×10^4 target cells were seeded in 96-well flat-bottom plates (Costar, Vitaris) and 4 h later 2.5×10^4 T cells (rested and washed) were added per well (i.e., at a 2:1 effector to target ratio) in complete medium. During the coculture period of the assay, no exogenous cytokines were added. To visualize target cell killing, Cytotox Red reagent (Essen Bioscience) was added at a final concentration of 125 nM in a total volume of 200 μL. Alternatively, a nuclei red PC3-PIP stable cell line expressing a nuclear restricted red fluorescent label was used for the assays. Negative controls comprising coincubation of UTD-T cells and tumor cells, as well incubation of tumor cells alone in the presence of Cytotox Red reagent to monitor spontaneous cell death, were included in all experiments. As a positive control to measure maximal killing tumor cells were treated with 1% triton solution. Images of total red area per well were collected every 2 h of the coculture and the total red area per well was analyzed with IncuCyte ZOOM software (Essen Bioscience). Data are expressed as the mean of different HDs ± SEM. venetoclax, Navitoclax, and A1155463 were resuspended according to the manufacturer's instructions and added in the coculture every 24 h at the reported working concentration.

Short-term cytotoxicity was evaluated by quantitative flow cytometric analysis. Briefly, 1×10^5 target cells were seeded in 96-well U-bottom plates (Costar, Vitaris) and rested T cells added at a 1:1 ratio for incubation at 37 °C for 5, 12, or 72 h. At each time point, cells were collected, washed, and stained with antibodies targeting CD3 and CD19, as well as a LIVE/DEAD marker (Thermo Fisher Scientific). Flow cytometry acquisition was kept at constant speed and normalized for the same time of sample running (30 s per tube). Residual live CD3$^-$CD19$^+$ target cells were quantified and used as the final readout.

Flow Cytometric Analysis. Transduced T cells were stained with A647 anti-mouse F(ab') monoclonal Ab (ImmunoJackson Research) to detect the R-chain and Fluorescein isothiocyanate anti-human c-Myc monoclonal Ab to detect the S-chain following overnight incubation with venetoclax. Near-infrared fluorescent reactive dye (APC-Cy-7) was used to assess viability (Invitrogen, Life Technologies). Additional monoclonal Abs (BD Biosciences) used for phenotypic analysis included BV711 mouse-anti-human CD3, BV605 mouse-anti-human CD4, and APC-Cy-7-labeled anti-human CD8. Tumor cell-surface expression of PSMA, EpCAM, and CD19 were detected using PE-labeled anti-human-PSMA, anti-human-EpCAM, and anti-human-CD19 mAbs (Biolegend). Intracellular staining using the eBioscience Foxp3/TF Staining Buffer Set was performed according to the manufacturer's instructions. Data acquisition and analysis were done with a BD FACS LSRII and FACS DIVA software.

Flow Cytometry–Based Apoptosis Assay. The evaluation of apoptosis markers Annexin V and 7ADD in T cells upon exposure to venetoclax was performed by either coculturing 1×10^5 T cells with 1×10^5 target tumor cells in the presence of drug or vehicle, or by incubating the T cells alone for 24 h. This assay was done using the Apoptosis Detection Kit (BioLegend) according to the manufacturer's instructions.

Mice and In Vivo Studies. NOD scid gamma mouse (NSG) mice were bred and housed in a specific and opportunistic pathogen-free animal facility in the Epalinges Campus of the Department of Oncology at the University of Lausanne. All cages housed five animals in an enriched environment providing unhindered access to food and water. Mice were monitored at least every other day for signs of distress during experiments and scarified at the endpoint by carbon dioxide overdose following Swiss Federal Veterinary Office guidelines and Cantonal Veterinary Office approval.

In Vivo Drug Toxicity Testing. NSG male mice aged 8 to 12 wk were shaved on the right flank and treated daily with 50 μL subcutaneous injections of venetoclax [2.5 mg/kg in Phosphate buffered saline (PBS) and 2% DMSO] or vehicle (2% DMSO in PBS). To assess the drug's effect on tumor control, five mice per group received subcutaneous injections of 5×10^6 PC3-PIP tumor cells. Once tumors were palpable (day 4), daily peritumoral injections of 2.5 mg/kg or 5 mg/kg of venetoclax or vehicle were administered. Tumor volume was measured every other day using calipers, with volumes calculated using $V = 1/2(\text{length} \times \text{width}^2)$.

Subcutaneous Therapeutic Prostate Tumor Model. To assess the therapeutic potential of iON-CAR-T and iONØ-CAR-T cells, 8 to 12-wk-old male NSG mice were injected subcutaneously with 5×10^6 tumor cells. Once palpable (day 5), mice were grouped based on mean tumor volume and SD and then treated by peritumoral injections of 2×10^6 T cells (at a 1:1 ratio of $CD4^+$ and $CD8^+$ T cells), including UTD, 2G-CAR, and iON or iONØ-CAR T cells (normalized for CAR expression; typically 40% for $CD4^+$ and 20% for $CD8^+$ T cells). Two hours post ACT, mice received peritumoral injections of venetoclax (2.5 mg/kg, Selleckchem), administered daily until the endpoint. Tumor volume was measured every other day using calipers.

Statistical Analysis. Data for CAR T cell experiments are presented as mean ± SEM. Statistical significance was determined using two-way ANOVA and one-way ANOVA test with post hoc Tukey correction according to the type of experiment and multiple comparison was also applied among all groups or functional coupled group, and specified in the figure legends. GraphPad Prism 10.0 (GraphPad Software) was utilized for statistical calculations, with significance levels set at $P \leq 0.05$ (*), $P \leq 0.01$ (***), $P \leq 0.001$ (***), and $P \leq 0.0001$ (****).

Data, Materials, and Software Availability. All study data are included in the article and/or *SI Appendix*.

ACKNOWLEDGMENTS. M.I. was supported by the Swiss NSF (SNSF# 310030_204326), the University of Lausanne, Ludwig Cancer Research, the Fondazione Teofilo Rossi di Montelera e di Premuda, the Swiss Institute for Experimental Cancer Research (ISREC) Foundation and the Prostate Cancer Foundation. BC was supported by the SNSF, the National Centres of Competence in Research (NCCR) in Chemical Biology and in Molecular Systems Engineering, an European Research Council (ERC) starting grant (#716058), and the Swiss Cancer League (KFS-5032-02-2020). L.S. was supported by the Strategic Focus Area "Personalized Health and Related Technologies (#2021-446)" of the ETH Domain and the Anniversary Foundation of Swiss Life for Public Health and Medical Research. We wish to thank members of the Flow Cytometry Platform and the Animal Care Facility of the Epalinges Campus of the University of Lausanne (UNIL) for their excellent support of our research. We thank Prof. Caroline Arber and Dr. Jan A. Rath (CHUV Hospital and UNIL) for sharing their BV173, Daudi, and CD19 knockout BV173 cells. We thank George Coukos (Ludwig Institute for Cancer Research, UNIL and CHUV hospital) for his advice and support of this work.

Author affiliations: [a]Ludwig Institute for Cancer Research Lausanne, Department of Oncology, University of Lausanne and Lausanne University Hospital, Lausanne 1011, Switzerland; [b]Institute of Bioengineering, École Polytechnique Fédérale de Lausanne, Lausanne 1011, Switzerland; and [c]Swiss Institute of Bioinformatics, Lausanne 1011, Switzerland

1. K. M. Cappell, J. N. Kochenderfer, Long-term outcomes following CAR T cell therapy: What we know so far. *Nat. Rev. Clin. Oncol.* **20**, 359–371 (2023).
2. F. Del Bufalo *et al.*, GD2-CART01 for relapsed or refractory high-risk neuroblastoma. *N. Engl. J. Med.* **388**, 1284–1295 (2023).
3. G. M. P. Giordano Attianese, S. Ash, M. Irving, Coengineering specificity, safety, and function into T cells for cancer immunotherapy. *Immunol. Rev.* **320**, 166–198 (2023).
4. C. DeSelm *et al.*, Low-dose radiation conditioning enables CAR T cells to mitigate antigen escape. *Mol. Ther.* **26**, 2542–2552 (2018).
5. F. G. Herrera *et al.*, Low-dose radiotherapy reverses tumor immune desertification and resistance to immunotherapy. *Cancer Discov.* **12**, 108–133 (2022).
6. E. Lanitis, D. Dangaj, M. Irving, G. Coukos, Mechanisms regulating T-cell infiltration and activity in solid tumors. *Ann. Oncol.* **28**, xii18–xii32 (2017).
7. E. Stefanidis *et al.*, Combining SiRPalpha decoy-coengineered T cells and antibodies augments macrophage-mediated phagocytosis of tumor cells. *J. Clin. Invest.* **134**, e161660 (2024).
8. E. Lanitis *et al.*, Optimized gene engineering of murine CAR-T cells reveals the beneficial effects of IL-15 coexpression. *J. Exp. Med.* **218**, e20192203 (2021).
9. J. Corria-Osorio *et al.*, Orthogonal cytokine engineering enables novel synthetic effector states escaping canonical exhaustion in tumor-rejecting CD8(+) T cells. *Nat. Immunol.* **24**, 869–883 (2023).
10. E. Lanitis, G. Coukos, M. Irving, All systems go: Converging synthetic biology and combinatorial treatment for CAR-T cell therapy. *Curr. Opin. Biotechnol.* **65**, 75–87 (2020).
11. R. G. Majzner, C. L. Mackall, Clinical lessons learned from the first leg of the CAR T cell journey. *Nat. Med.* **25**, 1341–1355 (2019).
12. B. Wolf *et al.*, Safety and tolerability of adoptive cell therapy in cancer. *Drug Saf.* **42**, 315–334 (2019).
13. J. Appelbaum *et al.*, Drug-regulated CD33-targeted CAR T cells control AML using clinically optimized rapamycin dosing. *J. Clin. Invest.* **134**, e162593 (2024).
14. G. Giordano-Attianese *et al.*, A computationally designed chimeric antigen receptor provides a small-molecule safety switch for T-cell therapy. *Nat. Biotechnol.* **38**, 426–432 (2020).
15. V. Stein, Synthetic Protein Switches: Theoretical and Experimental Considerations. *Methods Mol. Biol.* **1596**, 3–25 (2017).
16. C. Y. Wu, K. T. Roybal, E. M. Puchner, J. Onuffer, W. A. Lim, Remote control of therapeutic T cells through a small molecule-gated chimeric receptor. *Science* **350**, aab4077 (2015).
17. W. H. Leung *et al.*, Sensitive and adaptable pharmacological control of CAR T cells through extracellular receptor dimerization. *JCI Insight* **5**, e124430 (2019).
18. B. Salzer *et al.*, Engineering AvidCARs for combinatorial antigen recognition and reversible control of CAR function. *Nat. Commun.* **11**, 4166 (2020).
19. A. Fegan, B. White, J. C. Carlson, C. R. Wagner, Chemically controlled protein assembly: Techniques and applications. *Chem. Rev.* **110**, 3315–3336 (2010).
20. C. U. Zajc *et al.*, A conformation-specific ON-switch for controlling CAR T cells with an orally available drug. *Proc. Natl. Acad. Sci. U.S.A.* **117**, 14926–14935 (2020).
21. M. Jan *et al.*, Reversible ON- and OFF-switch chimeric antigen receptors controlled by lenalidomide. *Sci. Transl. Med.* **13**, eabb6295 (2021).
22. T. Miyamoto *et al.*, Rapid and orthogonal logic gating with a gibberellin-induced dimerization system. *Nat. Chem. Biol.* **8**, 465–470 (2012).
23. H. Schellekens, Factors influencing the immunogenicity of therapeutic proteins. *Nephrol. Dial. Transplant* **20**, vi3-9 (2005).
24. Z. B. Hill, A. J. Martinko, D. P. Nguyen, J. A. Wells, Human antibody-based chemically induced dimerizers for cell therapeutic applications. *Nat. Chem. Biol.* **14**, 112–117 (2018).
25. S. Carbonneau *et al.*, An IMiD-inducible degron provides reversible regulation for chimeric antigen receptor expression and activity. *Cell Chem. Biol.* **28**, 802–812.e6 (2021).
26. J. Kale, E. J. Osterlund, D. W. Andrews, BCL-2 family proteins: Changing partners in the dance towards death. *Cell Death Differ.* **25**, 65–80 (2018).
27. J. Lopez, S. W. Tait, Mitochondrial apoptosis: Killing cancer using the enemy within. *Br. J. Cancer* **112**, 957–962 (2015).
28. A. Shamas-Din, J. Kale, B. Leber, D. W. Andrews, Mechanisms of action of Bcl-2 family proteins. *Cold Spring Harb. Perspect. Biol.* **5**, a008714 (2013).
29. V. S. Marsden, A. Strasser, Control of apoptosis in the immune system: Bcl-2, BH3-only proteins and more. *Annu. Rev. Immunol.* **21**, 71–105 (2003).
30. F. J. Kohlhapp *et al.*, Venetoclax increases intratumoral effector T cells and antitumor efficacy in combination with immune checkpoint blockade. *Cancer Discov.* **11**, 68–79 (2021).

31. L. Grosse-Hovest *et al.*, Tumor-growth inhibition with bispecific antibody fragments in a syngeneic mouse melanoma model: The role of targeted T-cell co-stimulation via CD28. *Int. J. Cancer* **80**, 138–144 (1999).
32. J. N. Kochenderfer *et al.*, Construction and preclinical evaluation of an anti-CD19 chimeric antigen receptor. *J. Immunother.* **32**, 689–702 (2009).
33. B. Omer *et al.*, A costimulatory CAR improves TCR-based cancer immunotherapy. *Cancer Immunol. Res.* **10**, 512–524 (2022).
34. H. Liu *et al.*, Monoclonal antibodies to the extracellular domain of prostate-specific membrane antigen also react with tumor vascular endothelium. *Cancer Res.* **57**, 3629–3634 (1997).
35. S. P. Santoro *et al.*, T cells bearing a chimeric antigen receptor against prostate-specific membrane antigen mediate vascular disruption and result in tumor regression. *Cancer Immunol. Res.* **3**, 68–84 (2014).
36. J. Charo *et al.*, Bcl-2 overexpression enhances tumor-specific T-cell survival. *Cancer Res.* **65**, 2001–2008 (2005).
37. M. Jan, A. S. Sperling, B. L. Ebert, Cancer therapies based on targeted protein degradation–Lessons learned with lenalidomide. *Nat. Rev. Clin. Oncol.* **18**, 401–417 (2021).
38. B. Z. Stanton, E. J. Chory, G. R. Crabtree, Chemically induced proximity in biology and medicine. *Science* **359**, eaao5902 (2018).
39. L. Labanieh *et al.*, Enhanced safety and efficacy of protease-regulated CAR-T cell receptors. *Cell* **185**, 1745–1763.e22 (2022).
40. A. H. Long *et al.*, 4–1BB costimulation ameliorates T cell exhaustion induced by tonic signaling of chimeric antigen receptors. *Nat. Med.* **21**, 581–590 (2015).
41. E. W. Weber *et al.*, Transient rest restores functionality in exhausted CAR-T cells through epigenetic remodeling. *Science* **372**, eaba1786 (2021).
42. Y. G. Lee *et al.*, Modulation of BCL-2 in Both T cells and tumor cells to enhance chimeric antigen receptor T-cell immunotherapy against cancer. *Cancer Discov.* **12**, 2372–2391 (2022).